Design and Fabrication of a Miniature AC -Susceptibility Coil-Set Compatible for a Close-Cycle Refrigerator(CCR)

Ayan Pattanayek

Indian Institute of Science Education and Research Pune fulfilment
of the requirements for the degree of
MS-Quantum Technology Degree

Supervisor: Prof. Ashna Bajpai

Department of Physics
Indian Institute of Science Education and Research Pune
Dr. Homi Bhabha Road, Pashan, Pune 411008, INDIA.

Certificate of Examination

This is to certify that the dissertation titled **Design and Fabrication of a Miniature AC -Susceptibility Coil-Set Compatible for a Close-Cycle Refrigerator(CCR)** submitted by **Ayan Pattanayek** for the partial fulfilment of the MS-Quantum Technology Degree programme of the institute, has been examined by the thesis committee duly appointed by the institute. The committee finds the work done by the candidate satisfactory and recommends that the report be accepted.

[**Prof. Ashna Bajpai**]
(Supervisor)

[**Prof. Mukul Kabir**]
(Advisory Member)

Declaration

The work presented in this dissertation has been carried out by me under the guidance of Prof. Ashna Bajpai at the Indian Institute of Science Education and Research, Pune.

This work has not been submitted in part or in full for a degree, a diploma, or a fellowship to any other university or institute. Whenever contributions of others are involved, every effort is made to indicate this clearly, with due acknowledgement of collaborative research and discussions. This thesis is a bonafide record of original work done by me and all sources listed within have been detailed in the bibliography.

[**Ayan Pattanayek**]

Acknowledgements

I would like to thank my supervisor, Prof.Ashna Bajpai, for her guidance, valuable suggestions and continuous support throughout the course of this work. Her advice and encouragement played a crucial role in the successful completion of this thesis.

I would also like to thank Ajad Kumar, a PhD scholar, for his guidance in instrumentation.

I am grateful to my lab members and friends for their support, discussions, and motivation during challenging times.

Finally, I thank everyone who directly or indirectly contributed to the successful completion of this work.

.

Abstract

In this work, a coil set for ac susceptibility measurement was designed and fabricated, which is compatible with a Close-Cycle Refrigerator. This coil system consists of one primary coil and two secondary coils wound on a sapphire tube. The purpose of this miniature coil set is to assess the feasibility of detecting magnetic phase transitions at cryogenic temperatures, particularly below 77K, with a focus on weak antiferromagnetic transitions. This thesis also presents a literature survey on Kitaev candidates such as $RuCl_3$ and Na_2IrO_3.

Chapter 1 of the thesis introduces magnetic materials, including paramagnets, ferromagnets, and antiferromagnets. Chapter 2 details the experimental methods related to this project, including the working of CCR and the principles of ac susceptibility. Chapter 3 presents a short literature survey on quantum spin liquids and Kitaev magnets such as $RuCl_3$ and Na_2IrO_3. Chapter 4 presents design and fabrication details of the miniature coil set-up, wound on a sapphire tube during the course of this project. The sapphire tube was attached to a Cu flange that could be fitted and thermally anchored to the cold finger of CCR. Chapter 4 also presents room temperature data on the offset signal of secondary coils, with and without the copper flange. Chapter 5 presents offset data as a function of temperature when the miniature coil set was fitted inside the CCR. Results of test runs on $RuCl_3$ single crystal as well as ferromagnetic Ni samples are presented in this chapter. Overall, these data indicate that it is difficult to detect antiferromagnetic transitions using this miniature coil setup in the presence of a huge background signal. Detection of a ferromagnetic signal can be a possibility. However, even for tracking the ferromagnetic transitions, more experiments are needed to understand the origin of the background signal and its frequency dependence.

List of Figures

List of Tables

Contents

Chapter 1

Introduction

Studying the magnetic properties of materials at low temperatures is an important area of condensed matter physics. In quantum materials, magnetic properties and phase transition behaviour become prominent only at cryogenic temperatures. One of the most important experimental techniques used to investigate such properties is AC-susceptibility measurement, which allows the sensitive detection of magnetic phase transitions.

In this work, a miniature AC-susceptibility coil system was designed and fabricated to perform magnetic measurements inside a Closed Cycle Refrigerator (CCR). The AC-susceptometer consists of a primary coil and two secondary coils, connected in series opposition. Applying AC-current in the primary coil, generates an alternating magnetic field, while the secondary coils detect the magnetic response of the sample placed inside one of the secondary coils. The induced voltage in the secondary coil is proportional to the material's magnetic response.

This compact coil system was fabricated such that it could fit inside the limited space of CCR. For this purpose, a sapphire base cylindrical tube has been used to widen the coil set. This sapphire cylindrical tube was attached to the copper(Cu) block, which can be coupled with the cold finger of the Close-Cycle Refrigerator(CCR). A lock-in amplifier is also used to detect the induced voltage of the secondary coil. This thesis also presents a literature survey on quantum materials $RuCl_3$ and Na_2IrO_3.

In this chapter, the fundamentals of magnetisation and magnetic materials, which are important for understanding quantum materials, are discussed.

1.1 Magnetisation of the Material

Magnetism in materials originates from the physical quantity called magnetic momentum (µ). When an external magnetic field is applied to the materials, it has an associated energy, which is given by:

$$E = -\mu \cdot B$$

That means the magnetic moment tends to align in the direction of the applied magnetic field to minimise the energy.

Magnetisation of a material mainly depends on two factors: the electron spin magnetic moment and the orbital magnetic moment. We imagine the electron spin as a tiny charged particle that is spinning about its own axis. The orbital motion of the electron is also similar to the charge that is moving in a circular path around the nucleus. This combination of both effects gives us the total magnetic moment of the materials.

When a large number of atoms are present in a material, the combination of all magnetic moments produces the magnetisation (M). Magnetisation is defined as the total magnetic moment per unit volume of the material.[ref 1.]

1.1.1 Magnetic Susceptibility

Magnetic susceptibility measures how easily a material becomes magnetised when an external magnetic field (H) is applied. In the case of magnetic material, the magnetic field can be written as B and H. The relation between these two vectors

$$\mathbf{B} = \mu_0 (\mathbf{H} + \mathbf{M})$$

where μ_0 is called the permeability of free space. [ref 2.]

For linear material, magnetisation is proportional to the applied magnetic field-

$$\mathbf{M} = \chi \mathbf{H}$$

Where χ is called magnetic susceptibility. When an AC magnetic field is applied, the magnetic response of the material can be expressed in two components: one is the real component, and the other is the imaginary component.

For the AC magnetic field, this χ is written as-

$$\chi(\omega) = \chi'(\omega) + i\chi''(\omega) \tag{1.1}$$

Where $\chi'(\omega)$ is real part. $\chi''(\omega)$ is imaginary part.

1.2 Heisenberg Model and the Concept of Exchange Interaction

The magnetic properties of the material come from the spin and orbital angular momentum of the electron. In many magnetic materials, spin interaction between two electrons is the dominant contribution to magnetism.

The most important theoretical model that describes the spin interaction is the Heisenberg model. This model explains the origin of magnetic ordering in solids. The Heisenberg model is based on several assumptions, such as that the interactions only depend on the neighbouring spin, only consider spin interaction, neglecting orbital motion part, spin interaction is the same in all directions, etc.

1.2.1 Exchange Interaction

Direct Exchange Interaction

Direct exchange interaction occurs when the electron orbitals of two magnetic ions overlap directly without the involvement of any intermediate atom. The strength of this type of interaction depends on two factors: the distance between two atoms and the overlap of the orbits.[ref 2.]

The Heisenberg Hamiltonian can define the direct exchange interaction energy-

$$H = -J\,\mathbf{S}_i \cdot \mathbf{S}_j$$

Where J is the exchange interaction constant.

- If $J > 0$, Ferromagnetic (FM) alignment.
- If $J < 0$ Antiferromagnetic (AFM) alignment.

.

Supper Exchange Interaction

Supper exchange interaction is an indirect magnetic interaction that happens between two magnetic intermediate atoms. This happens usually in transition-metal oxides, where an oxygen atom separates the magnetic ions. The superexchange interaction is

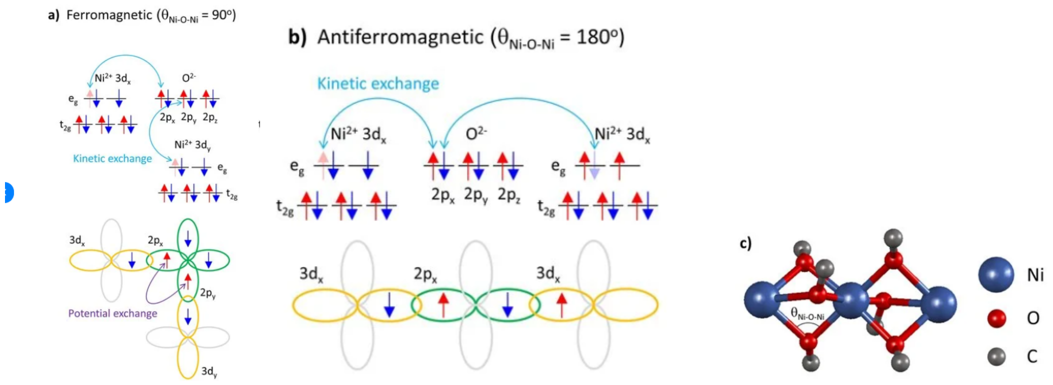

Figure 1.1: This figure shows the superexchange interaction between the Ni 3d orbits via oxygen 2p orbitals [ref 3]

usually antiferromagnetic. When multiple types of interaction happen simultaneously, the antiferromagnetic one is generally dominant.

In Figure a, the sharing of electrons happens in a way that follows Hund's rule, which ensures the maximum spin multiplicity in the oxygen 2p orbitals. This results in a ferromagnetic exchange interaction between the nearest neighbours of Ni ions. In Figure b., the kinetic exchange due to the overlapping Ni and Oxygen orbits leads to the antiferromagnetic superexchange interaction.

Double Exchange Interaction

Double exchange interaction is a kind of magnetic exchange that can happen between ions that have different oxidation states.

In the first stage of the double exchange process, oxygen donates one electron to the Mn^{4+} ion. In the next stage, the empty orbital can be filled by an electron from a neighbouring Mn^{3+} ion.

As a result of these two steps, an electron has effectively moved from the Mn^{3+} ion to the Mn^{4+} ion through the oxygen atom. This kind of process is called double exchange interaction, as shown in Figure [1.2]

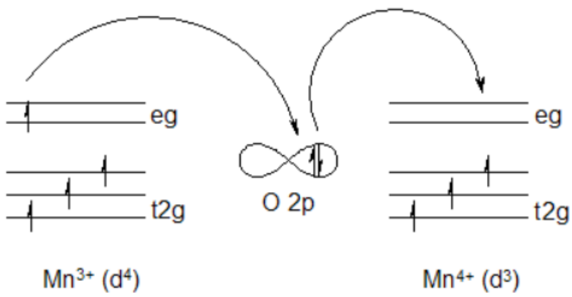

Figure 1.2: Example of double exchange in the compound $La_{1-x}A_xMnO_3$ [ref 4]

1.3 Spin Ordering in Magnetic Materials

1.3.1 Diamagnetic Material

Diamagnetism is a property of a material where an applied magnetic field creates an induced magnetic field in the opposite direction, which is why a repulsive force occurs. The magnetic susceptibility of a diamagnetic material is negative. Diamagnetism is present in all materials, and always makes a weak contribution to the magnetic response.

Examples of diamagnetic materials are NaF, NaCl, KBr, etc.

1.3.2 Paramagnetic Material

Paramagnetism occurs in atoms or ions that contain an unpaired electron. In the absence of the external magnetic field, the magnetic moments are in random directions. For this material, ignoring the exchange interaction terms because the magnetic moments of the atoms do not interact sufficiently.

When an external magnetic field is applied, the magnetic moment tries to align in the applied field direction. This produced a small positive magnetisation in the material. The magnetic susceptibility of a paramagnetic material is positive.

The magnetic susceptibility of the paramagnetic material is temperature-dependent, which is defined as -

$$\chi = \frac{C}{T}$$

Where C is called the curie constant, and T is called the temperature.

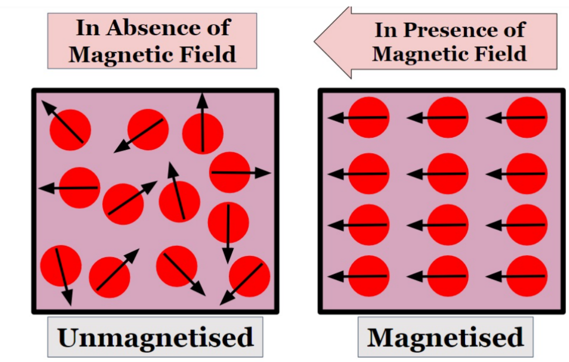

Figure 1.3: Paramagnetism [ref 2]

Examples of paramagnetic materials are aluminium, platinum, etc.

1.3.3 Ferromagnetic Material

In the case of ferromagnetism, when the temperature is below a specific point, the nearby atoms automatically line up in the same direction on their own, without needing any external magnetic field. This specific temperature is known as the critical temperature, and it marks the change between the ferromagnetic state and the paramagnetic state, as shown in Figure[1.5].

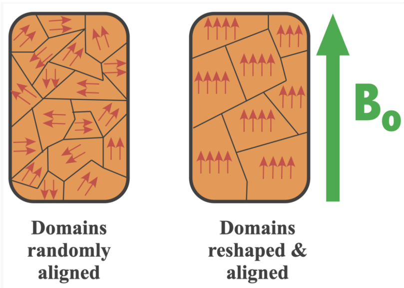

Figure 1.4: Ferromagnetism [ref 5]

When an external magnetic field B is applied in a ferromagnetic material, then the Hamiltonian should be- [ref 2]

$$\hat{H} = -\sum_{j,k} J_{j,k}\, \mathbf{S}_j \cdot \mathbf{S}_k + g\mu_B \sum_j \mathbf{S}_j \cdot \mathbf{B} \tag{1.2}$$

Where $J_{j,k}$ is the exchange interaction constant. If $J_{j,k} > 0$, then it's a ferromagnetic interaction, and the second term is called the Zeeman energy.[ref 2]

At $T > T_C$, the magnetic susceptibility for this material is-

$$\chi \propto \frac{1}{T - T_C}$$

1.3.4 Anti-ferromagnetic Material

In antiferromagnets, the individual magnetic dipoles are oriented in a way such that the bulk of the material has a vanishing total magnetisation. For an antiferromagnetic material, the exchange interaction constant $J_{j,k}$ should be negative. Antiferromagnetic order may exist, sufficiently at low temperature, but vanishes at and above the Neel temperature. Above the Neel temperature, the material is typically paramagnetic. Magnetic susceptibility of an antiferromagnetic material above the Neel temperature is defined as-

$$\chi \propto \frac{1}{T + T_N} \tag{1.3}$$

Where T_N is the Neel temperature.

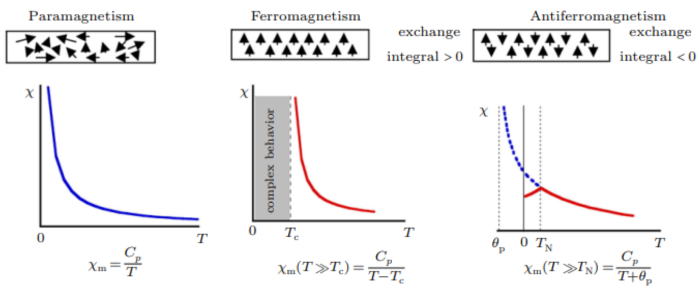

Figure 1.5: magnetic susceptibility for paramagnetic, ferromagnetic and antiferromagnetic materials as a function of temperature.[ref 6]

Examples of antiferromagnetic materials are NiF_2, MnO, α-Fe_2O_3, CoF_2, etc.

1.3.5 Ferrimagnetic Material

In the case of ferrimagnetic material, the magnetic moments are also aligned in a similar way to antiferromagnetic material, but the moments have unequal magnitudes, as shown in Figure[1.7]. So the spontaneous magnetisation remains. In ferrimagnetic materials, magnetism is lost above a certain temperature. This temperature is called the Curie temperature.

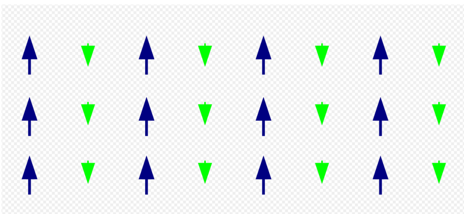

Figure 1.6: Ferrimagnetism [ref 2]

Examples of the ferrimagnetic materials are Fe_3O_4, $NiFe_2O_4$, $MgFe_2O_4$.

1.3.6 Spin Glass Material

In the case of a spin glass material, the magnetic moment of the atom is randomly oriented and becomes frozen in a random direction at low temperature. At high temperatures, a spin glass system behaves like a paramagnetic material. As the temperature decreases, the magnetic moments eventually freeze into a disordered but stable pattern at a characteristic temperature known as the freezing temperature.

There are so many unique properties, such as the slow relaxation of magnetisation and frequency-dependent susceptibility peak, etc are present in the spin glass system.

Examples of spin glass systems are CuMn, AuFe, AgMn, etc.

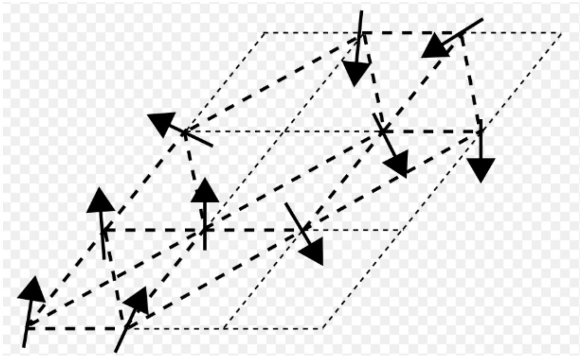

Figure 1.7: Magnetic moment of spin glass material[ref 26]

In Chapter 3, we discuss about the Kitaev model and its role in quantum materials. We also discussed the properties of quantum spin-liquid materials such as $RuCl_3$ and Na_2IrO_3.

Chapter 2

Experimental Methods and Instrumentation

In this chapter, the working principle of the AC-susceptometer, the Close-Cycle refrigerator and the Lock-in amplifier are discussed.

2.1 Working Principle of AC-Susceptometer

AC susceptibility measurement is a powerful technique for measuring the magnetic signal. It is useful for studying materials such as superconductors, spin glasses, and quantum spin liquids.

The AC-susceptometer consists of a three-coil system, one primary coil and two identical secondary coils. These two secondary coils are wound in series opposition. When there is no sample inside the secondary coils, they cancel each other's signal. But when a magnetic sample is placed inside a secondary coil, this symmetry is broken, and the sample's magnetic signal is obtained. [ref 2.]

Magnetic susceptibility means how easily a material is magnetised. In the DC field, magnetic susceptibility can be written as-

$$\chi = \frac{M}{H}$$

In the AC field, it can be written as-

$$\chi = \frac{dM}{dH}$$

In the AC field, magnetic susceptibility is defined as how magnetisation changes with changing field. Sometimes the magnetic response of the signal is linear and sometime its non-linear. Mathematically, it can be written as-

$$M = M_0 + \chi^{(1)}H + \chi^{(2)}H^2 + \chi^{(3)}H^3 + \cdots$$

Where $\chi^{(1)}$ is called linear susceptibility, and higher order terms are called non-linear susceptibility.

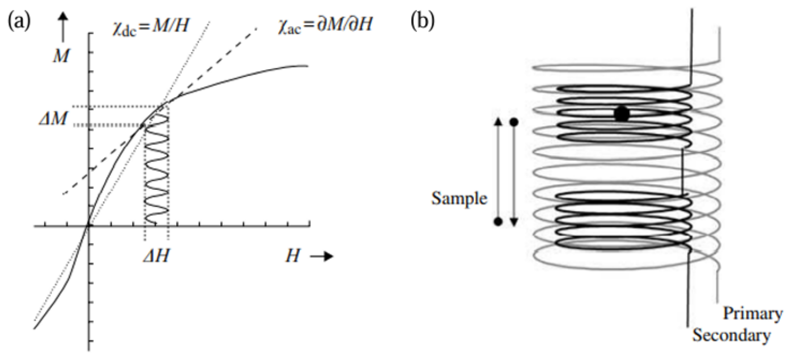

Figure 2.1: 1. M-H curve of AC and DC susceptibility. 2. Block diagram of AC-susceptometer [ref 2]

2.2 Working Principle of Close-Cycle Refrigerator (CCR) and Experimental Application in this Work

The Close-Cycle Refrigerator(CCR) is used to achieve and maintain the cryogenic temperature. The CCR system is working in a closed-loop configuration using helium(He) gas. The CCR operates based on the compression and expansion of the helium gas.

First, helium (He) gas is compressed using an external compressor. When the gas is compressed, its temperature increases. This hot, high-pressure gas is then passed through a heat exchanger, where it is cooled down by removing excess heat using water.

After cooling, the high-pressure helium (He) enters the cold head of the system. Here, the gas expands, and its temperature drops significantly due to the Joule-Thomson effect, which is the process where a gas cools when it expands.

This cold helium gas then flows to the cold stage, where the sample is placed. It absorbs heat from the sample.

Figure 2.2: 1.A closed-cycle cryostat that has a radiation shield, vacuum shroud, cold head, compressor, and hoses. 2. Sapphire base ac coil attached to the cold finger of the CCR

Finally, the helium (He) gas returns to the compressor, where it is compressed again, and the whole process repeats. Since this is a closed cycle, no helium is lost during the operation. This continuous cycle allows the sample to reach and maintain a low temperature without using liquid helium (He).

In this work, the sapphire base AC coil sample holder is mounted onto the cold finger of the CCR. The temperature of the cold finger varied from room temperature to a few kelvin, and the temperature dependence of the magnetic behaviour of QSL materials will be investigated.

2.3 Lock-in Amplifier Working Principle and Signal Detection

A lock-in amplifier is used to measure small AC signals by converting them into a DC output, which is proportional to the signal amplitude. The lock-in amplifier extracts weak signals even in the presence of significant noise. The core component of the lock-in amplifier is a phase-sensitive detector (PSD), which converts the AC signal to a DC signal.

The block diagram of the lock-in amplifier is shown in Figure [2.3]. The working principle of a lock-in amplifier is explained step by step below.

Signal Channel

The input signal typically consists of the desired signal and unwanted noise. This initial signal passes through an AC-coupled amplifier for adjustable gain. In this coupling process, they remove the DC offset signal and allow the AC component to be processed. This adjustable gain amplifier is amplifying the signal, that is why its amplitude matches the input range of the phase-sensitive detector(PSD) for accurate detection.

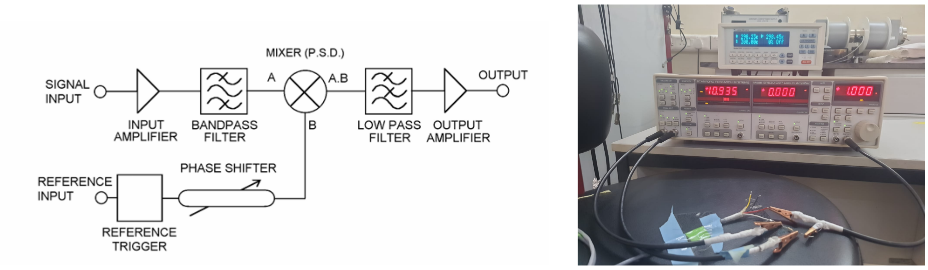

Figure 2.3: 1. Block diagram of a lock-in amplifier.[ref 23] 2. SR830 DSP model lock-in amplifier

Reference Channel

In the ideal situation, a high-level, stable, and noise-free reference signal is directly available in the experiment. In this case, generating the reference signal is relatively straightforward. In a practical case, the available reference signal is noisy and not perfectly symmetric. In this case, an internal reference signal of the lock-in amplifier is used. The internally generated reference goes through a phase shifter, which is used to correct any phase differences that may have occurred between the signal and reference inputs during the experiment, before it is applied to the PSD.

Phase Sensitive Detector (PSD)

There are two common methods of implementing the PSD: these are an Analog Multiplier and a Digital Multiplier.

Use of Analog Multiplier and Digital Multiplier

In the case of an analog multiplier, the PSD multiplies the input signal by the reference signal of the same frequency. It is simple in principle, but in the presence of a large, noisy signal, which reduces the noise rejection as a result detect the lower accuracy signal.

In the digital multiplier approach, the input signal is passed through an analogue-to-digital converter. This converter transforms the input analogue signal into a digital signal, then multiplies it by the digital reference signal. This method gives high accuracy and stability.

Low Pass Filter

The low-pass filter removes the AC component from the output of the PSD, and it only allows the DC components of the signal. Typically, an RC-type filter is used in this case.

Output

The final output of the lock-in amplifier is a DC signal whose amplitude is proportional to the signal amplitude. In modern instruments, the output is digital, although an analog base-voltage output is also available.

In lock-in amplifier detection, there are two components, which are in-phase components(X)and out-of-phase components(Y).

In this work, measure R instant of X, where R is

$$R = \sqrt{X^2 + Y^2}$$

We also use a temperature sensor (Cernox CX-1030-SD) to measure the temperature of the sample holder, which is connected to the temperature connector.

Using this measurement instrument, we try to measure the magnetic signal of the quantum material as a function of temperature.

Chapter 3

Literature Survey: $RuCl_3$ and Na_2IrO_3

In quantum materials, collective behaviour exists, such as high-temperature superconductivity, topological phases, and exotic magnetic states. These properties of the quantum material are promising for future technology applications.

The key feature of the quantum material is strong electron correlation and spin-orbit coupling. Due to this strong electron correlation, a complex ground state is created that cannot be explained by using classical theory. Spin-orbit coupling creates unusual magnetic properties for heavy materials.

$RuCl_3$ and Na_2IrO_3 are called quantum materials because of their complex geometry and strong electron correlation. They also show the bond-dependent anisotropic magnetic interaction, which is explained in the Kitaev model.

In this chapter, we discussed about the structure and the magnetic properties of the quantum material. The basic theory of the Kitaev model is also explained here.

3.1 Theoretical Background of the Quantum Spin Liquid Material (QSL)

In the case of normal magnetic material, the spins are aligned in an ordered pattern, such as ferromagnetic and antiferromagnetic materials. But for QSL materials, the spins do not align in an ordered pattern, there is no long-range magnetic ordering due to strong quantum fluctuation.

3.1.1 Magnetic Fluctuation

Magnetic fluctuation occurs when the spins are not aligned in a simple order pattern because of the complex geometry. [ref 24]

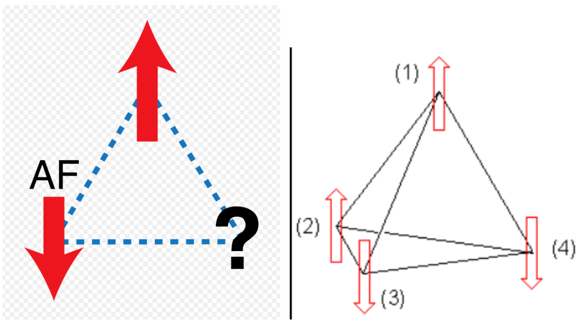

Figure 3.1: 1. Spin fluctuation of the triangular lattice. 2. Spin fluctuation for the tetrahedron lattice structure.[ref 23]

For a triangular lattice of three spins with antiferromagnetic interaction, if one spin point is up and the second spin point is down, then the third spin cannot simultaneously satisfy the condition of its neighbours. For this fluctuation, the spin is not settled down into a unique ground state. Instantly, it has many configurations of the same energy, and the spins are fluctuating between them, as shown in Figure [3.1].

For a ferromagnetic material, the ground state can be written as-

$$|\psi_{\mathrm{FM}}\rangle = |\uparrow\uparrow\uparrow\uparrow \ldots\rangle \tag{3.1}$$

Similarly, for an antiferromagnetic material, the ground state can be written as-

$$|\psi_{\mathrm{AFM}}\rangle = |\uparrow\downarrow\uparrow\downarrow \ldots\rangle \tag{3.2}$$

In the case of QSL materials, the spins do not behave independently.

For the triangular lattice, they create a quantum entangled ground state, which is written as [ref 27]-

$$|\psi_{\text{singlet}}\rangle = \frac{1}{\sqrt{2}}\left(|\uparrow\downarrow\rangle - |\downarrow\uparrow\rangle\right) \tag{3.3}$$

In materials such as $RuCl_3$ and Na_2IrO_3, spin fluctuation occurs not only for the complex geometry but also for the bond-dependent interaction, which is explained in the Kitaev model.

3.1.2 Spin-Orbit Coupling

An electron has two motions: spin motion and orbital motion. Spin-orbit coupling arises due to the interaction between these two properties. This interaction Hamiltonian can be written as-

$$H_{\text{SOC}} = \lambda\, \mathbf{L} \cdot \mathbf{S} \tag{3.4}$$

Where λ is called the coupling strength, L is called the orbital motion of the electron, and S is called the electron spin motion.

For the strong spin-orbit coupling, they create a degenerate ground state. The magnetic properties of the QSL materials depend on this degenerate ground state.

3.1.3 Kitaev Model

The Kitaev model is the most important theoretical model to explain the QSL behaviour. It is defined on a two-dimensional honeycomb lattice, where magnetic ions are arranged in a hexagonal structure. [ref 9.]

In this model, the spin interaction between neighbouring spins is direction-dependent. The Hamiltonian of the Kitaev model is written below-

$$H = -K\left(\sum_{\langle i,j\rangle_x} S_i^x S_j^x + \sum_{\langle i,j\rangle_y} S_i^y S_j^y + \sum_{\langle i,j\rangle_z} S_i^z S_j^z\right) \tag{3.5}$$

Where K is the interaction strength.

So the single spin is connected to the multiple neighbours. As a result, spins do not satisfy all the interaction conditions simultaneously. For that, the system does not develop long-range magnetic ordering.

Therefore, the Kitaev model gives us the fundamental framework for the theoretical understanding of QSL materials, such as $RuCl_3$ and Na_2IrO_3.

3.2 Origin of Quantum Spin Liquid(QSL) Behavior: $RuCl_3$ and Na_2IrO_3

3.2.1 Crystal Structure of $RuCl_3$ and Na_2IrO_3

α-$RuCl_3$ is one type of layer material; its structure is mainly made in a two-dimensional sheet. Each sheet contains Ru^{3+} ions arranged in a hynicomb structure.

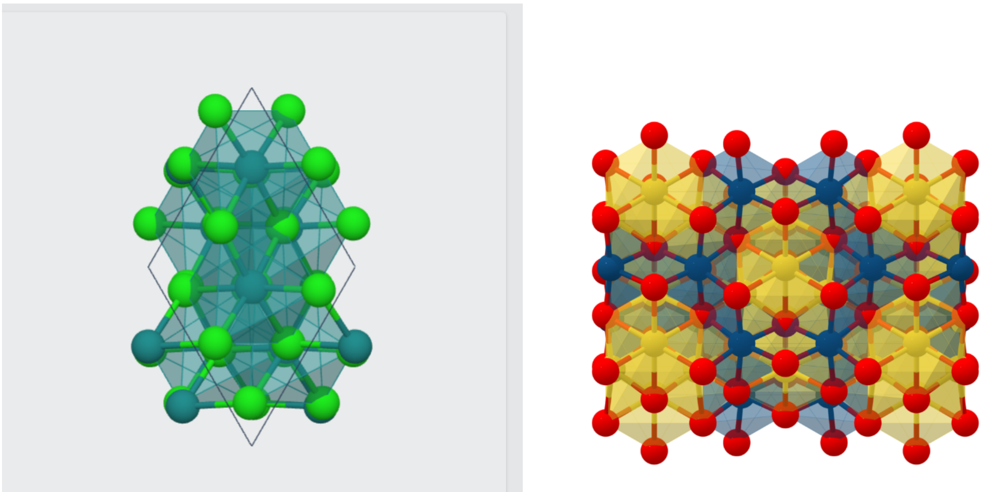

Figure 3.2: 1. Crystal structure of 2D (layered) α-$RuCl_3$, central atoms (dark) Ru and outer atoms (green) Cl. 2. Crystal structure of 2D (layered) Na_2IrO_3, red sphere represents O^{2-}, blue sphere represents transition-metal ions, yellow sphere represents Na^+ ions.[ref 24]

Each Ru^{3+} ion is surrounded by six Cl^- ions; they are creating a $RuCl_6$ octahedron, which is a two-dimensional honeycomb lattice. This Complex geometry is important for the spin fluctuation.

Similarly, Na_2IrO_3 also has a layered 2D honeycomb lattice. Oxygen atoms surround each Ir ion, forming IrO_6 octahedra. For this complex geometry, magnetic spin fluctuation occurs. That's why these two materials are called quantum spin liquid materials.

3.2.2 Strong-Spin Orbit Coupling of $RuCl_3$ and Na_2IrO_3

In $RuCl_3$ and Na_2IrO_3 materials, they have heavy atoms, such as rubidium(Ru) and iridium (Ir). These heavy magnetic ions, Ru^{3+} and Ir^{4+}, have partially filled 5d-orbitals, so the spin-orbital coupling is strong.

Inside the crystal, each heavy ion is surrounded by atoms(Cl^- and O^{2-}), forming an octahedral environment. Due to the partially filled 5d-orbits, the energy level splits into two parts; one state is called the ground state (t_{2g}), and another state is called the higher energy state (e_g). Due to the strong spin-orbit coupling, the t_{2g} state splits into two parts, which can be described by effective spin $j_{\text{eff}} = \frac{1}{2}$. That's why the magnetic properties do not depend on the spin only; they depend on the spin-orbit entanglement state. [ref 19]

3.2.3 Bond Dependent Interaction of $RuCl_3$ and Na_2IrO_3

In $RuCl_3$ and Na_2IrO_3 materials, due to the complex geometry and strong spin-orbit coupling, the magnetic interaction between the neighbouring spins is highly anisotropic.

This bond-dependent interaction is explained in the Kitaev model. Due to the anisotropic interaction, spins are strongly fluctuating, and it is impossible to minimise the interaction energy simultaneously. Instantly, they may host a highly entangled ground state, such as a quantum spin liquid state.

3.2.4 Magnetic Ordering of $RuCl_3$ and Na_2IrO_3

In the absence of an external magnetic field, the system exhibits long-range magnetic ordering at low temperature. As the temperature is reduced, the material undergoes a magnetic phase transition at the transition temperature. The transition temperature of the α-$RuCl_3$ material is nearly 7K [ref 12]. Below this temperature, Ru^{3+} ions no longer fluctuate freely, instead arrange themselves in an ordered pattern.

Below this temperature, the spins try to order in a zigzag antiferromagnetic pattern of α-$RuCl_3$ material as shown in Figure[2.3]

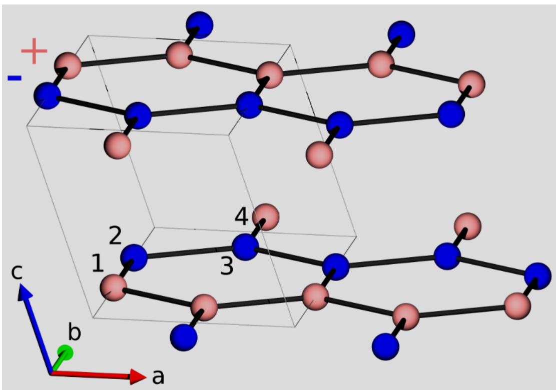

Figure 3.3: Zigzag antiferromagnetic ordering [ref 26]

Due to this magnetic ordering, the magnetic signal is increasing at the transition point. Singh and Gegenwart reported that the honeycomb lattice material Na_2IrO_3, where zigzag antiferromagnetic ordering is observed nearly at 15K.[ref 13]

Chapter 4

Design and Fabrication of a Miniature AC-Susceptometer Compatible with a Close Cycle Refrigerator(CCR)

An AC susceptometer consists of a primary coil and two secondary coils; these two secondary coils are wound in series opposition. This coil setup is miniature, such that it can be fitted in the limited sample space of CCR. For a CCR-based AC susceptometer, several challenges exist, including space constraints, thermal coupling, and minimising noise.

In this chapter, the design, fabrication and calibration procedure of the AC-susceptometer are discussed in detail.

4.1 Material Selection and Designing

4.1.1 Cylindrical Sapphire Tube Design

A sapphire tube for winding the primary and secondary coils were used because sapphire is non-magnetic and has high thermal conductivity for low-temperature measurement.

The total length of the sapphire cylinder was 28 mm, as indicated in Figure[4.1]. This sapphire cylinder structure was symmetrically divided into three portions for the coil configuration. One side of the sapphire cylinder will be attached to the copper(Cu) block. Here, the primary coil is wound over a 20 mm length, as indicated in Figure[4.1]. Two secondary coils were wound over a 5 mm length; they are geometrically identical,

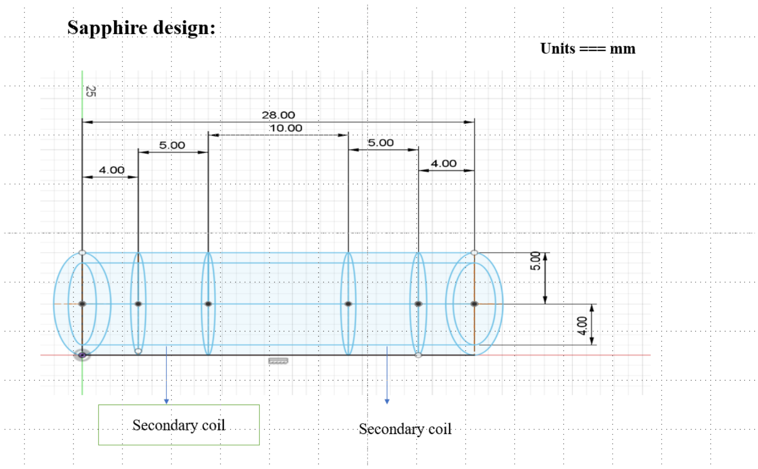

Figure 4.1: Cylindrical sapphire tube design

and a 10 mm gap was maintained between them.

4.1.2 Copper(Cu) Block Sample Holder Design

The non-magnetic copper(Cu) material was selected due to its high thermal conductivity, which ensures that the effective heat transfer for the cold finger of the CCR to the coil system. This efficient thermal coupling allows the sample and coil system to quickly reach and maintain the desired cryogenic temperature with minimal thermal gradients.

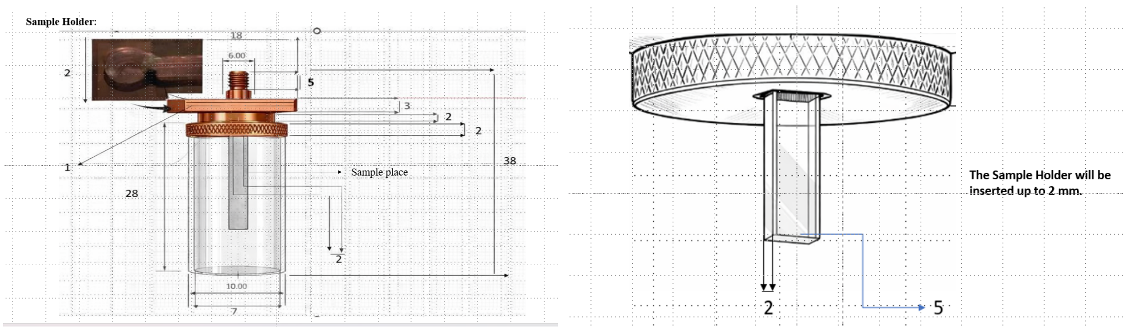

Figure 4.2: Copper(Cu) block sample holder design

The upper portion of the copper(Cu) block consists of a flange structure that will directly screw with the cold finger of the closed-cycle refrigerator(CCR). This provides high thermal coupling and mechanical stability. The length and width of the flange portion were 5 mm and 6 mm, respectively, as shown in Figure[4.2]. A 2 mm depth cavity was created in the copper(Cu) block for the sapphire-based sample plate. This sapphire plate can be inserted in the Copper(Cu) block up to 2 mm to ensure good thermal contact, and it will allow the sample to cool down to the cryogenic temperature. The outer radius of the cylindrical sapphire was 5 mm; therefore, a

5 mm ring-shaped cavity was also created in the Copper(Cu) block to mount this sapphire cylinder. This sapphire cylinder can be inserted up to 3 mm to ensure thermal contact and allow the coil system to cool down to cryogenic temperatures. A small space was created in the copper(Cu) block to place the Cernox sensor, which measures the actual temperature of the sample holder. The total length of the sample holder was 38 mm, and this entire system (consisting of a sapphire tube and a copper flange) will be integrated into the CCR.

4.1.3 Hylum Ring

Hylum rings were used to support the winding of the secondary pickup coils in the AC susceptibility probe. Hylum was chosen because it is non-magnetic and a good electrical insulator. Four Hylum rings were used for this setup, as shown in Figure [4.3]. The diameter and width of the hylam rings were 10.8 mm and 1 mm.

4.2 Fabrication of Coil System and Construction of Sample Mounting Sapphire Plate

An AC-susceptometer consists of a primary coil and two secondary coils. These two secondary coils are geometrically identical, and they are connected in a series opposition connection to cancel out the background signal. When a sample is placed in the one secondary coil, and a measurable magnetisation signal is obtained. The details of the fabrication process are explained below.

4.2.1 Fabrication Process

Initially, a 28mm sapphire tube was cut using a cutting machine, and after that, it was cleaned using ethanol to remove the surface impurity.

Primary Coil Winding

The primary coil was wound on the cylindrical sapphire tube, whose outer diameter(OD) is 10 mm. The primary coil was wound over a 20 mm length. It was wound using 36 SWG copper wires. It consists of two layers of winding, with 193 turns in one layer and 194 turns in the other layer, giving a total of 387 turns.

A manual coil winding machine was used to wind the coil. The resistance of the primary coil is $R = 3.5\,\Omega$ at room temperature.

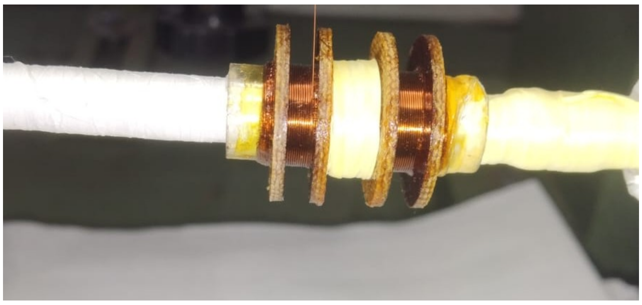

Figure 4.3: Primary coil winding

Parameter	**Value**
Number of turns in primary coil	387
Layers of winding in the primary coil	2
Number of turns in each layer	193 and 194
primary coil resistance	3.8 Ω

Table 4.1: Experimental parameters and measured values of the primary coil at room temperature.

Secondary Coil Winding

The secondary pickup coils were wound on top of the primary coil. The coils have a length of 4 mm and are separated by a distance of 10 mm. The secondary coils were wound using 46 SWG copper wire to increase the number of turns within this small space and consist of 1000 turns in each coil. These layers were supported at the ends using Hylum rings of diameter 10.8 mm and width 1 mm.

Figure 4.4: 1. Secondary pickup coil winding, 2. Sapphire base AC coil system with copper block sample holder

The resistance of the two secondary pickup coils is 102 Ω and 103.8 Ω at room temperature. After winding these two coils using a coil winding machine, using a lock-in amplifier, apply an AC current to the primary coil, which is connected in series with a 1 Ω resistance, and check the induced voltage in each secondary coil at room temperature. The induced voltage in each pickup coil is 9.78 mV and 9.41 mV for a 1V sin input. This date shows that these bridges are nearly identical. These two coils are connected in series opposition, and they can cancel out the background signal. When a sample is placed in the one secondary coil, the magnetisation signal is obtained. The total resistance of the two pickup coils after connection is 203.0 Ω at room temperature. However detecting linear and non-linear AC-susceptibility in Quantum materials(AFM) remains a challenge.

Parameter	**Value**
Length of each secondary coil	4 mm
Number of turns in each secondary coil	1000
Each secondary coil resistance	102 Ω and 102.3 Ω
Induce voltage in each secondary coil for a 1V input applied to the primary coil	9.67 mV and 9.88 mV

Table 4.2: Experimental parameters and measured values of the secondary coil at room temperature.

Sapphire Base Sample Rod Construction

The sample is mounted in the sapphire base plate, which is shown in Figure[4.5]. This sapphire plate is inserted in the copper(Cu) block up to 2 mm to ensure good thermal contact and allow the sample to cool down to the cryogenic temperature. The total length of the sample rod is 32 mm.

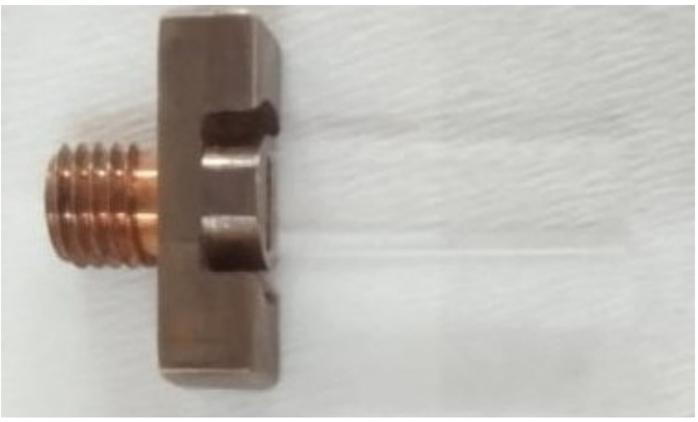

Figure 4.5: Sapphire base sample plate

In this system, the sample is placed in the lower secondary coil.

4.3 Working Principle and Measurement Technique of an AC Susceptometer

The primary coil is connected to the sine out of the SR830 DSP model lock-in amplifier. The alternating voltage applied to the primary coil generates an oscillatory magnetic field that induces a magnetic response in the sample. The secondary coil is connected between the signal input of the lock-in amplifier (A and B modes).

The real and imaginary components of the magnetic susceptibility are determined using the lock-in amplifier by setting the reference signal in phase with the magnetic field generated by the primary coil. This is achieved by adjusting the reference to be in phase with the voltage measured across the 1 Ω resistor. The oscillatory magnetic field in the primary coil is proportional to the current flowing through it, and the current is proportional to the voltage across the 1 Ω resistor; the reference signal is effectively tracked in the applied magnetic field [ref. 2].

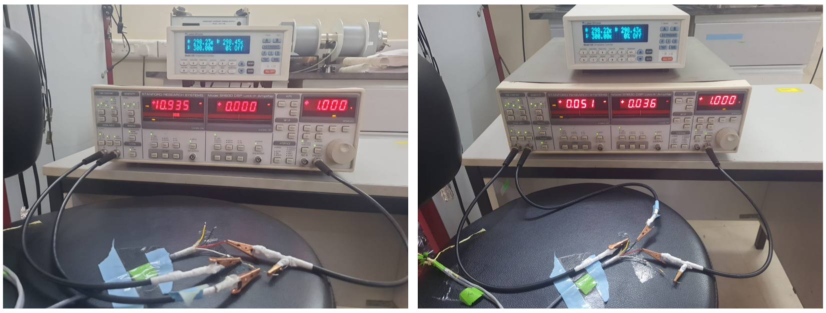

Figure 4.6: Connection of the lock-in measurement 1. across 1 Ω resistance. 2. secondary coil connection

The induced voltage in the secondary coil depends on the rate of change of magnetic flux

$$v(t) = -\frac{d\Phi}{dt}$$

When the sample is placed in the one secondary coil, there symmetry is broken, and the sample's magnetic response is detected in the lock-in amplifier. In this work, we detect R instant of X and Y. Where R represents the magnitude of the detected signal, which is a combination of both X and Y components.

$$R = \sqrt{X^2 + Y^2}$$

To get an accurate result, a background measurement is taken before each run. In this case, the measurement is done without a sample, but the sample rod and all other things, like the temperature sensor, are placed in the same position as before. So this dry run helps us to measure the unwanted signal. So the final signal is obtained by subtracting this offset from the with sample measurement.

4.4 Performance Testing of the AC-Susceptometer at Room Temperature

The performance of the AC-susceptibility coil system was evaluated by measuring the induced voltage in the pickup coil as a function of input voltage in the primary coil at room temperature. The measurement was done in both cases with a copper(Cu) block sample holder and without a copper(Cu) block sample holder.

This experimental measurement data demonstrates that the induced voltage in the secondary coil is directly proportional to the applied input voltage of the primary coil. This linear behaviour comes from Faraday's law of electromagnetic induction; the induced voltage depends on how fast the magnetic flux changes.

A significant difference was observed in the absence of the copper(Cu) block, where the induced voltage is higher, but in the presence of the copper(Cu) block, where the induced voltage is slightly lower, which is shown in fig [4.7].

The overall linear relationship between input voltage and induced voltage, and a small induced signal in the range of a few microV, confirms that the AC-susceptibility coil system is working properly and cancels the background signal at room temperature.

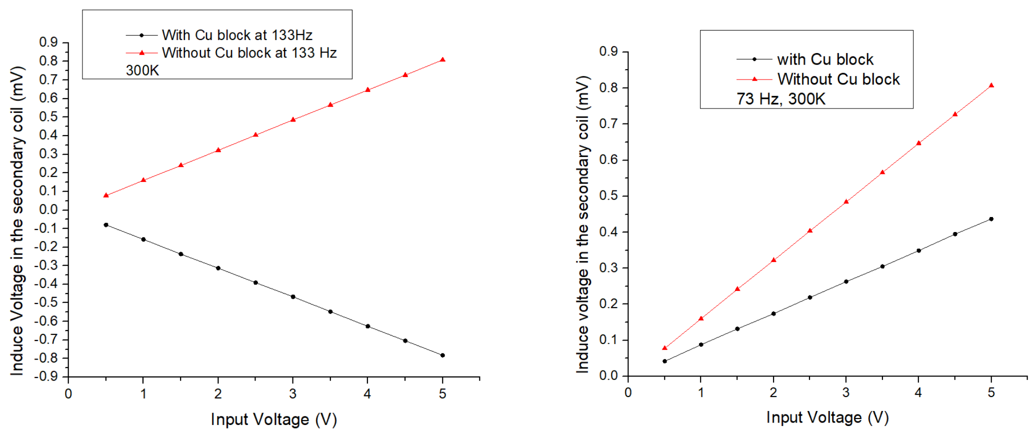

Figure 4.7: Real Component(X) of the induced voltage in pickup coil as a function of input voltage at room temperature

4.5 Mounting of the Miniature Coil Set in CCR

1. The outer vacuum shroud and inner radiation shield of the CCR were removed after releasing the vacuum. The miniature coil-set sample holder was mounted to the cold finger of the Close-Cycle Refrigerator(CCR). The two primary coil wires and the two secondary coil wires were connected with the CCR's wires. After the connection, the resistance of the primary coil and secondary coil are 33.8 and 234 Ω, respectively. This additional resistance comes from the CCR wires. All the connected wires were thermally anchored using GE varnish. Thereafter, the inner radiation and outer vacuum shroud of CCR are fitted back.

2. After evacuating the vacuum, the chillar and compressor are started, and the cooling process begins.

3. The ac susceptibility signal is measured with the sample inside one of the coils. Signal is also measured without a sample. Signal without sample data corresponds to offset, and it needs to be subtracted from the signal with sample inside one of the coils.

$$V_{\text{actual}} = V_{\text{with sample}} - V_{\text{offset}} \tag{4.1}$$

Chapter 5

Result and Discussion

5.1 Offset Measurement of the AC-Susceptometer

We first present the data of offset signal.

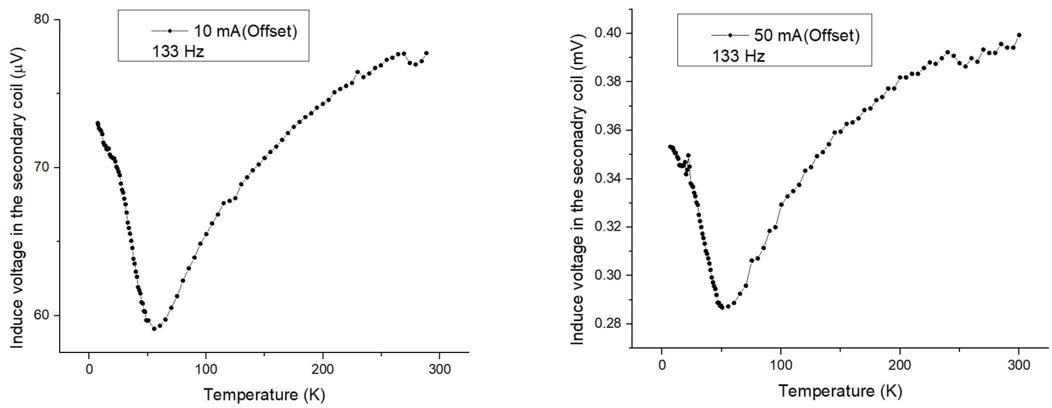

Figure 5.1: Offset data plot for 1. 10 mA and 2. 50 mA

This figure[5.1] shows how the offset is changing as a function of temperature for two different excitation currents, 10 mA and 50 mA. At room temperature, the offset is high, but as the temperature decreases, the offset signal also gradually decreases up to 50K, and below 50K, the signal increases again, producing a U-shape behaviour.

5.2 Measurements on a $RuCl_3$ Single Crystal

We made a test run on a $RuCl_3$ single crystal. This sample is obtained from Prof Yogesh Singh ab from IISER Mohali. The sample weight is 2.4 mg.

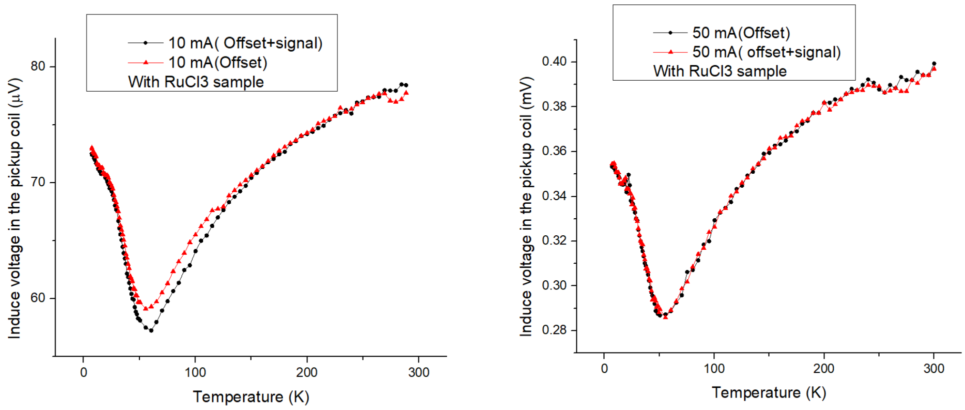

Figure 5.2: 1. With the $RuCl_3$ sample measuring at 10 mA (133 Hz). 2. With the $RuCl_3$ sample measuring at 50 mA (133 Hz).

After subtracting the offset from the with sample signal, we get the actual magnetic signal of the $RuCl_3$, as shown in the figure[5.3].

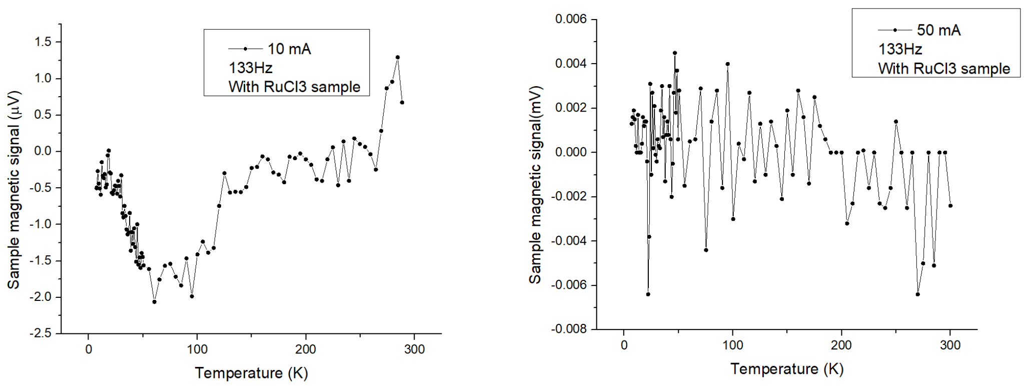

Figure 5.3: 1. Actual magnetic signal of the $RuCl_3$ sample at 10 mA. 2. Actual magnetic signal of the $RuCl_3$ sample at 50 mA.

Unfortunately, the magnetic transition point of the $RuCl_3$ sample can not be observed in this measurement, because the magnetic signal of the quantum material is extremely weak. As a result, the signal is dominated by the offset signal.

To verify the performance of the measurement system, use a ferromagnetic material which have large magnetic signal. Due to this large signal, the magnetic response of the material was clearly detected, which is shown in the figure[5.4].

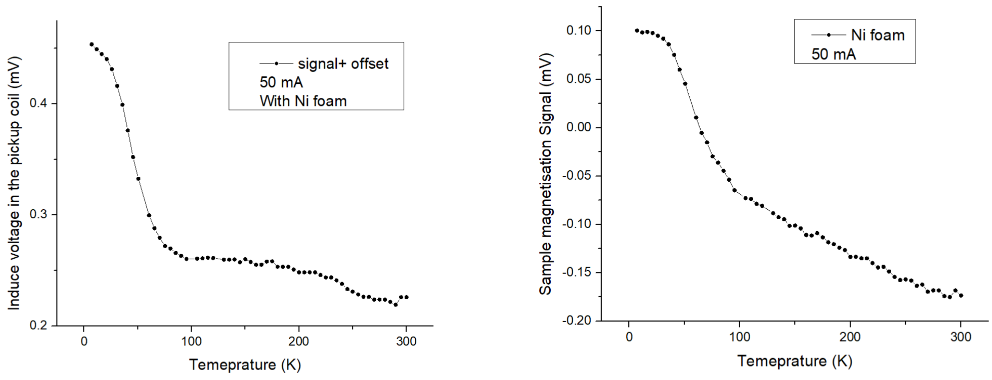

Figure 5.4: 1. Magnetic signal for Ni-foam 2. Actual magnetic signal of the Ni-foam at 50 mA (133 Hz).

Chapter 6

Conclusion

In the CCR base AC-susceptibility measurement, first, the background offset signal is carefully measured. It was observed that the offset signal strongly depended on the temperature and increased below 50K. There can be multiple sources of background signal in a CCR-based AC susceptibility setup. The room temperature data on the sapphire coil set shows the effect of the copper flange on the offset at the room temperature. This also shows significant frequency dependence. When such an assembly (sapphire tube +Cu Flange) is put inside CCR with various metallic parts, the nature of the offset signal as a function of temperature can vary significantly with temperature and frequency. Thus, more runs are needed for understanding the offset.

In the present coil set, it is not possible to measure a weak signal corresponding to antiferromagnetic correlations in Kitaev candidates. However, the data on ferromagnetic samples, such as Ni, appear more promising. The possibility of measuring ferromagnetic signal needs to be tested in samples that show ferromagnetic transition in the temperature range of CCR (5K-300K).

To improve the measurement, it is necessary to reduce the background signal and increase the number of turns of the secondary coil.

Chapter 7

Future Work

1. Reduce the background noise by removing the Cernox sensor from the setup because it was placed near the coil setup, which can give some unwanted signal.
2. Increase the sensitivity of the AC-spectrometer by increasing the number of tuners in the secondary.

Bibliography

1. Introduction to Magnetic Materials Author(s): B. D. Cullity, C. D. Graham First published:29 February 2008.

2. Probing ultra-slow magnetisation relaxation in transition metal fluorides through DC and AC magnetometry. IISER Pune MS Thesis- Shashwat Singh Tomar.

3. Kittel, Introduction to Solid State Physics, Wiley.

4. Exchange coupling in a frustrated trimetric molecular magnet reversed by a 1D nano-confinement† Oleg Domanov,a Eugen Weschke,b Takeshi Saito,c Herwig Peterlik,a Thomas Pichler,a Michael Eisterer,d Hidetsugu Shiozawa

5. V. Iacovacci, G. Lucarini, L. Ricotti, and A. Menciassi, "Magnetic field-based technologies for lab-on-a-chip applications," Lab-on-a-Chip Fabrication and Application, 2016. doi: 10.5772/62865.

6. Electrochromic magnetic properties of electrode materials for lithium ion batteries Guo Zheng-Fei , Pan Kun , Wang Xue-Jin

7. Antiferromagnetism. Theory of Suyerexchange Interaction P. W. ANDERsON BeII Telephone Laboratories, Murray IJN, Ewe Jersey (Received January 9, 1950)

8. Eminuscent phase in frustrated magnets: a challenge to quantum spin liquids S. V. Syzranov 1 A. P. Ramirez 1.

9. An introduction to Kitaev model-I Saptarshi Mandal1, 2 , and Arun M Jayannavar1, 2, † 1 Institute of Physics, P.O.: Sainik School, Bhubaneswar 751005, Odisha, India. 2Homi Bhabha National Institute, Mumbai - 400 094, Maharashtra, India (Dated: June 23, 2020)

10. A jeff = 1/2 Kitaev material on the triangular lattice: the case of NaRuO2 Aleksandar Razpopov 1, David A. S. Kaib 1, Steffen Backes 2,3,4, Leon Balents5, Stephen D. Wilson 6, Francesco Ferrari 1, Kira Riedl1 and Roser Valentí 1

11. Low-temperature crystal and magnetic structure of -RuCl3 H. B. Cao,1, A. Banerjee,1,† J.-Q. Yan,2,3 C. A. Bridges,4 M. D. Lumsden,1D. G. Mandrus,2,3 D. A. Tennant,5 B. C. Chakoumakos,1 and S. E. Nagler1,6

12. Magnetic order in -RuCl3: A honeycomb-lattice quantum magnet with strong spin-orbit coupling J. A. Sears,1 M. Songvilay,1 K. W. Plumb,1 J. P. Clancy,1 Y. Qiu,2,3 Y. Zhao,2,3 D. Parshall,2 and Young-June Kim1,*

13. article Singh2010, author = Singh, Yogesh and Gegenwart, Philipp, title = Antiferromagnetic Mott insulating state in single crystals of the honeycomb lattice material Na2IrO3, journal = Physical Review B, volume = 82, pages = 064412, year = 2010, doi = 10.1103/PhysRevB.82.064412

14. Generic Spin Model for the Honeycomb Iridates beyond the Kitaev Limit Jeffrey G. Rau,1 Eric Kin-Ho Lee,1 and Hae-Young Kee1,2,*

15. Spin-S Kitaev-Heisenberg model on the honeycomb lattice: A high-order treatment via the many-body coupled cluster method M. Georgiou , 1,* I. Rousochatzakis , 1,† D. J. J. Farnell , 2,‡ J. Richter , 3,§ and R. F. Bishop 4,1,

16. A snapshot review—Fluctuations in quantum materials: from skyrmions to superconductivity L. Shen1,2,3 · M. Seaberg2 · E. Blackburn3 · J. J. Turner1,2

17. Design of an A.C. susceptometer based on a cryocooler Ph. Vanderbemden University of Lie‘ge, S.U.P.R.A.S., Montefiore Electricity Institute, B28, Sart-Tilman, B-4000 Liege, Belgium

18. An Automated Ac Susceptibility Set up Fabricated Using a Closed-Cycle Helium Refrigerator S. Kundu and T. K. Nath* Department of Physics and Meteorology, Indian Institute of technology Kharagpur,

19. Quantum materials with strong spin–orbit coupling: challenges and opportunities for materials chemists. Alexander J. Browne, ORCID logo a Aleksandra Krajewska ORCID logo b and Alexandra S. Gibbs

20. Exchange Mechanisms in E. Pavarini, E. Koch, F. Anders, and M. Jarrell: Correlated Electrons: From Models to Materials, Jülich 2012, ISBN 978-3-89336-796-2

21. Magnetic properties refer to the response of a material to an applied magnetic field. Different materials react to the application of magnetic field differently.

22. A Frequency-Domain Description of a Lock-in Amplifier John H. Scofield Department of Physics, Oberlin College, Oberlin, OH 44074

23. REVIEW ARTICLE OPEN Experimental identification of quantum spin liquids Jinsheng Wen 1,2, Shun-Li Yu 1,2, Shiyan Li2,3, Weiqiang Yu4 and Jian-Xin Li1,2.

24. The Materials Project: A materials genome approach to accelerating materials innovation Free Anubhav Jain; Shyue Ping Ong; Geoffroy Hautier; Wei Chen; William Davidson Richards; Stephen Dacek; Shreyas Cholia; Dan Gunter; David Skinner; Gerbrand Ceder; Kristin A. Persson

25. Quantum spin liquid candidate as superior refrigerant in cascade demagnetization cooling Xin-Yang Liu1,2,8, Yuan Gao 1,2,8, Han Li 1,3, Wentao Jin1 , Junsen Xiang4, Hai Jin5, Ziyu Chen1 ,Wei Li 2,6, Gang Su 3.

26. Reference: Cannella, V., Mydosh, J. A. (1972). "Magnetic ordering in gold-iron alloys." Physical Review B, 6(11), 4220.

27. Quantum Spin Liquid Ground States of the Heisenberg-Kitaev Model on the Triangular Lattice. Pavel Kos Elite Master Program Theoretical and Mathematical Physics Ludwig–Maximilians–Universit¨at M¨unchen